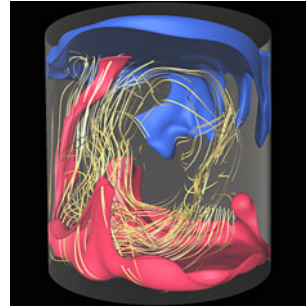$$\mathbb{F}^{\text{ocus}}_{\text{luids}}$$

Boundary layer structure in confined turbulent thermal convection

R. Verzicco†

Dipartimento di Ingegneria Industriale, Università di Roma
'Tor Vergata', via del Politecnico 1, 00133, Roma, Italy

Physics of Fluids, University of Twente, PO Box 217,
7500 AE Enschede, The Netherlands

The structure of viscous and thermal boundary layers at the heated and cooled plates in turbulent thermally driven flows are of fundamental importance for heat transfer and its dependence on the thermal forcing (the Rayleigh number Ra in non-dimensional form). The paper by Shi, Emran & Schumacher (*J. Fluid Mech.*, this issue, vol. 706, 2012, pp. 5–33) stresses the deviations of the boundary layer vertical profiles from the Prandtl–Blasius–Pohlhausen theory. Recent papers showing very similar results, in contrast, focus more on the similarities.

Key words: Bénard convection, boundary layer structure, buoyant boundary layers

1. Introduction

A typical model problem of natural convection is the Rayleigh–Bénard flow in which a fluid layer of thickness h is vertically bounded by two horizontal plates at different temperatures, the hotter being below the colder. If g is the magnitude of the acceleration due to gravity, $\Delta = T_{hot} - T_{cold}$ the temperature difference between the plates, α the isobaric thermal expansion coefficient and ν and κ, respectively, the kinematic viscosity and thermal diffusivity, then the flow is governed by the Rayleigh $Ra = g\alpha\Delta h^3/(\nu k)$ and Prandtl $Pr = \nu/k$ numbers. A third parameter is the geometrical aspect ratio of the tank $\Gamma = d/h$, where d is some relevant horizontal dimension. The response of the system is the specific heat transfer q that in non-dimensional form is represented by the Nusselt number $Nu = qh/(\lambda\Delta)$ (λ is the thermal conductivity of the fluid) and the strength of the flow is quantified by a velocity U or through the Reynolds number $Re = Uh/\nu$.

As the Rayleigh number increases the flow undergoes several transitions and it becomes eventually turbulent. The self-organization of the flow into large-scale structures induces a 'wind' sweeping the horizontal plates and generating viscous and thermal boundary layers. In the last two decades turbulent thermal convection has been investigated theoretically, numerically and experimentally and a wide range of the Ra–Pr–Γ parameter space has been spanned (see Ahlers *et al.* 2009 for a comprehensive review); the structures of the boundary layers have been extensively investigated although a consensus has not yet been reached.

† Email address for correspondence: verzicco@uniroma2.it

2. Overview

All the theoretical models, in one way or another, make assumptions on the boundary layers that can be satisfied to a greater or lesser extent.

Malkus ([1954](#)) predict $Nu \sim Ra^{1/3}$ by assuming that the heat transfer is independent of the thickness of the fluid layer, thus implying that the lower and upper boundary layers evolve independently of each other. Shraiman & Siggia ([1990](#)) assume a turbulent viscous boundary layer and a thermal boundary layer deeply nested within the viscous one ($Pr > 1$) to obtain the correlation $Nu \sim Ra^{2/7}$. Kraichnan ([1962](#)) for very large Rayleigh numbers ($Ra > Ra_T$) predicts an elusive asymptotic regime for arbitrary Prandtl number in the form $Nu \sim Ra^{1/2}/(\ln Ra)^{3/2}$ by using classical mixing-length arguments for a turbulent boundary layer.

Grossmann & Lohse ([2000](#)) proposed a unifying model that divides the Ra–Pr space into different regimes depending on the dominant contribution (boundary layer or bulk) to the energy and temperature variance dissipation rates and on the nature (laminar or turbulent) of the boundary layers. This model has predicted successfully the Nusselt and Reynolds numbers for a wide range of Ra and Pr. In this model the boundary layers have been assumed laminar and of Blasius type (Blasius [1908](#)), thus many recent investigations have focused their attention on the boundary layer structure.

It is worth mentioning that for this flow the thickness of the thermal boundary layer can be estimated as $\delta_T \simeq h/(2Nu)$. The thickness of the viscous boundary layer δ_v can be smaller than δ_T for $Pr < 1$ and vice versa for $Pr > 1$. Assuming the correlation $Nu \simeq 0.08Ra^{0.32}$ it is trivial to estimate that for $Pr = O(1)$ at $Ra = 10^8$ one obtains $\delta_T \approx \delta_v \simeq h/60$ and at $Ra = 10^{12}$ the result is $\delta_T \approx \delta_v \simeq h/1100$; the analysis of the boundary layer structure, therefore, requires large experimental setups (du Puits *et al.* [2007](#)) or high-resolution particle image velocimetry (Sun *et al.* [2008](#)) or high-fidelity direct numerical simulations (Shi, Emran & Schumacher [2012](#); Stevens *et al.* [2012](#)) for the highest Rayleigh numbers.

In the paper by Shi *et al.* ([2012](#)) the flow in a cylindrical cell of aspect ratio $\Gamma = 1$ at $Pr = 0.7$ is simulated for $Ra = 3 \times 10^9$ and $Ra = 3 \times 10^{10}$; the structure of the boundary layers has been analysed by collecting time series of temperature and velocity components on various vertical arrays for different positions over the plates. The main findings of this study are that the boundary layer vertical structure has some analogies with the Blasius profile although there are also evident differences. The quality of the agreement improves if a dynamic rescaling of the profiles with the time-dependent boundary layer thicknesses is performed as suggested in Zhou & Xia ([2010](#)). It is also found that the differences with respect to the Prandtl–Blasius solution are smaller for the lower value of Ra when the flow is smoother in space and less unsteady in time. The flow unsteadiness has two distinct sources. The first is the azimuthal tilting and twisting of the large-scale circulation (LSC) that changes the direction of the wind sweeping the plates. The second reason for the unsteadiness is the emission of thermal plumes from the plates that tend to generate wall-normal velocity components inducing additional velocity orthogonal to the main plane of the wind. The plume emission is followed by a recovery phase in which the flow becomes more steady.

The above results, summarized in figure [1](#)(*a,b*), are not surprising if one recalls that the Blasius solution holds for a steady, laminar, strictly two-dimensional flow over a flat plate with zero streamwise pressure gradient. In contrast, in the confined Rayleigh–Bénard flow the wind induced by the LSC is inherently three-dimensional and unsteady with wind velocity that is hardly parallel to the wall at any point. In
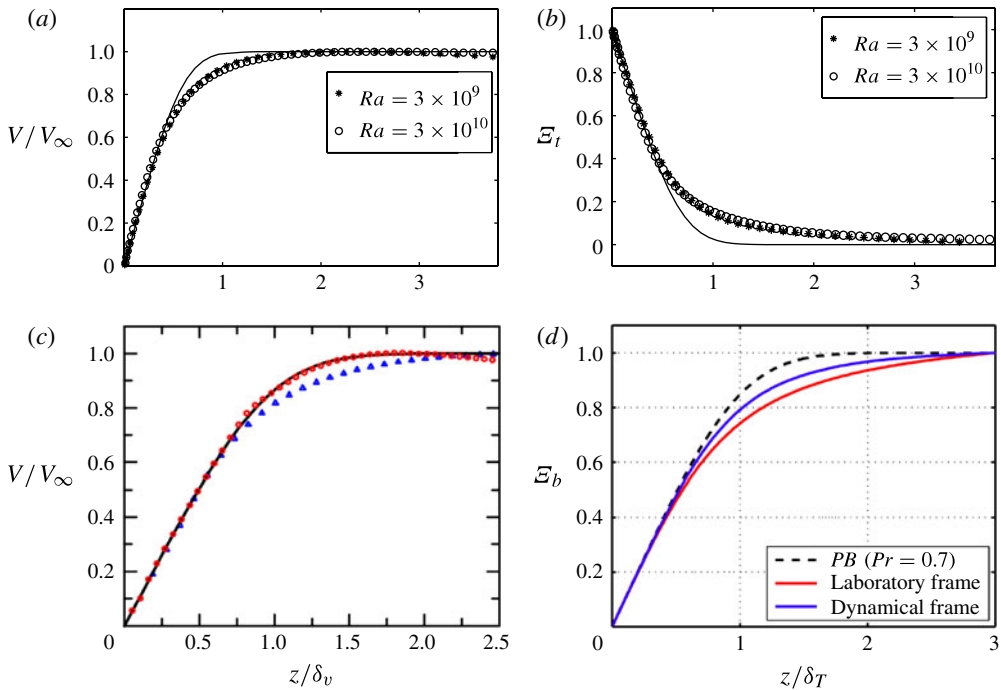
FIGURE 1. Vertical profiles of viscous and thermal boundary layers. (*a*,*b*) Probe array at the cell centre and upper plate, $Pr = 0.7$ and a cylindrical cell of $\Gamma = 1$ (adapted from Shi *et al.* 2012). The solid lines show the Prandtl–Blasius solution. (*c*) Array near the centre of the bottom plate at $Pr = 4.3$ and $Ra = 1.9 \times 10^{11}$. The cell is a parallelepiped with width/height $\Gamma \simeq 1$ and depth/height $\simeq 1/4$. Blue triangles: 'raw' data (laboratory frame); red circles: coordinate rescaled with the instantaneous boundary layer thickness (dynamical frame) (adapted from Zhou & Xia 2010, copyright (2010) by the American Physical Society). (*d*) Array near the centre of the bottom plate at $Pr = 0.7$, $Ra = 2 \times 10^{12}$ and a cylindrical cell of $\Gamma = 1/2$ (*PB*: Prandtl–Blasius) (adapted from Stevens *et al.* (2012), copyright (2012) by the American Physical Society). $\Xi_t = (T_m - T(z))/(T_m - T_{cold})$, $\Xi_b = 1 - (T_m - T(z))/(T_m - T_{hot})$.

addition, the horizontal flow is generated by the vertical hot/cold current that bends at the plates and bends again after having swept them; this phenomenon is accompanied by a streamwise pressure gradient that, in fact, is found in the numerical simulations by Shi *et al.* (2012). In view of how different the conditions of the Rayleigh–Bénard flow are with respect to the Blasius boundary layer it is surprising how much the boundary layer profiles resemble each other. This statement is reinforced by observing that in a laboratory setup it is not trivial to reproduce the Blasius boundary layer profile over a flat plate owing to small disturbances and pressure gradients that are difficult to suppress (Schlichting 1979).

3. Future

There are several papers (e.g. Zhou & Xia 2010 and Stevens *et al.* 2012) which for the same problem report boundary layer vertical profiles with the same level of agreement with the Prandtl–Blasius solution as the present study, even if the

previous work tends to focus more on the similarities. Two examples are shown in figure 1(*c,d*) and indeed it can be appreciated that the results are very similar and that in the region closest to the wall the profiles are always indistinguishable. It seems that rather than different results there are different interpretations; this point however deserves further investigation. When the Rayleigh number exceeds a threshold ($\approx 10^{13}$) there are indications that the transition to turbulence of the boundary layers occurs (Gauthier & Roche 2008); in view of the possible appearance of the asymptotic state (Kraichnan 1962) it would be crucial to characterize the structure and the dynamics of the boundary layers in this regime. The extreme thinness of the boundary layers poses difficult challenges to the experimental techniques while numerical simulations need to use the largest computers now available to attack this parameter range. Another point deserving investigation is the structure of the boundary layers in the presence of background rotation that introduces the Rossby number as additional input and increases the complexity of the physics with the Ekman and Stewartson layers (Kunnen *et al.* 2011). All these topics are being clarified thanks to the combination of theoretical models, laboratory experiments and numerical simulation all involved in the joint effort to unravel the complex dynamics of the turbulent Rayleigh–Bénard flow.

References

AHLERS, G., GROSSMANN, S. & LOHSE, D. 2009 Heat transfer and large-scale dynamics in turbulent Rayleigh–Bénard convection. *Rev. Mod. Phys.* **81** (2), 503–537.

BLASIUS, H. 1908 Grenzschichten in Flüssigkeiten mit keiner Reibung. *Z. Math. Phys.* **56**, 1–37.

GAUTHIER, F. & ROCHE, P.-E. 2008 Evidence of a boundary layer instability at very high Rayleigh number. *Europhys. Lett.* **83**, 24005.

GROSSMANN, S. & LOHSE, D. 2000 Scaling in thermal convection: a unifying theory. *J. Fluid Mech.* **407**, 27–56.

KRAICHNAN, R. H. 1962 Turbulent thermal convection at arbitrary Prandtl number. *Phys. Fluids* **5**, 1374–1389.

KUNNEN, R. P. J., STEVENS, R. J. A. M., OVERKAMP, J., SUN, C., VAN HEIJST, G. J. F. & CLERCX, H. J. H. 2011 The role of Stewartson and Ekman layers in turbulent rotating Rayleigh–Bénard convection. *J. Fluid Mech.* **688**, 422–442.

MALKUS, M. V. R. 1954 Heat transport and spectrum of thermal turbulence. *Proc. R. Soc. Lond.* A **225**, 196–212.

DU PUITS, R., RESAGK, C., TILGNER, A., BUSSE, F. H. & THESS, A. 2007 Structure of thermal boundary layers in turbulent Rayleigh–Bénard convection. *J. Fluid Mech.* **572**, 231–254.

SCHLICHTING, H. 1979 *Boundary Layer Theory*. McGraw-Hill.

SHI, N., EMRAN, M. S. & SCHUMACHER, J. 2012 Boundary layer structure in turbulent Rayleigh–Bénard convection. *J. Fluid Mech.* **706**, 5–33.

SHRAIMAN, B. I. & SIGGIA, E. D. 1990 Heat transport in high Rayleigh number convection. *Phys. Rev.* A **42**, 3650–3653.

STEVENS, R. J. A. M., ZHOU, Q., GROSSMANN, S., VERZICCO, R., XIA, K.-Q. & LOHSE, D. 2012 Thermal boundary layer profiles in turbulent Rayleigh–Bénard convection in a cylindrical sample. *Phys. Rev.* E **85**, 027301.

SUN, C., CHEUNG, Y.-H. & XIA, K.-Q. 2008 Experimental studies of the viscous boundary layer properties in turbulent Rayleigh–Bénard convection. *J. Fluid Mech.* **605**, 79–113.

ZHOU, Q. & XIA, K.-Q. 2010 Measured instantaneous viscous boundary layer in turbulent Rayleigh–Bénard convection. Rayleigh–Bénard convection in a cylindrical sample. *Phys. Rev. Lett.* **104**, 104301.